

Unparticle Physics in the Moller Scattering

İnanç Şahin* and Banu Şahin†

*Department of Physics, Faculty of Sciences,
Ankara University, 06100 Tandogan, Ankara, Turkey*

Abstract

We investigate the virtual effects of vector unparticles in the Moller scattering. We derive the analytic expression for scattering amplitudes with unpolarized beams. We obtain 95% confidence level limits on the unparticle couplings λ_V and λ_A with integrated luminosity of $L_{int} = 50, 500 \text{ fb}^{-1}$ and $\sqrt{s} = 100, 300$ and 500 GeV energies. We show that limits on λ_V are more sensitive than λ_A .

PACS numbers: 14.80.-j, 12.90.+b, 13.66.-a

*isahin@science.ankara.edu.tr

†dilec@science.ankara.edu.tr

I. INTRODUCTION

In his recent papers Georgi [1, 2] has proposed a new scenario. In his proposal new physics contains both Standard Model (SM) fields and a scale invariant sector described by Banks-Zaks (BZ) fields [3]. The two sectors interact via the exchange of particles with a mass scale M_U . Below this large mass scale interactions between SM fields and BZ fields are described by non-renormalizable couplings suppressed by powers of M_U [1, 4]:

$$\frac{1}{M_U^{d_{SM}+d_{BZ}-4}} O_{SM} O_{BZ} \quad (1)$$

The renormalization effects in the scale invariant BZ sector then produce dimensional transmutation at an energy scale Λ_U [5]. In the effective theory below the scale Λ_U , the BZ operators are embedded as unparticle operators. The operator (1) is now matched to the following form,

$$C_{OU} \frac{\Lambda_U^{d_{BZ}-d_U}}{M_U^{d_{SM}+d_{BZ}-4}} O_{SM} O_U \quad (2)$$

here, d_U is the scale dimension of the unparticle operator O_U and the constant C_{OU} is a coefficient function.

If unparticles exist, their phenomenological implications should be discussed. In the literature, there have been many discussions which investigate various features of unparticle physics [6]. In the some of these researches several unparticle production processes have been studied. Possible evidence for this scale invariant sector might be the signature of a missing energy. It can be tested experimentally by examining missing energy distributions.

Other evidence for unparticles can be explored by studying its virtual effects. Imposing scale invariance, the spin-1 unparticle propagator is given by [2, 7]:

$$\Delta(P^2)^{\mu\nu} = i \frac{A_{d_U}}{2\sin(d_U\pi)} (-P^2)^{d_U-2} \left(-g^{\mu\nu} + \frac{P^\mu P^\nu}{P^2} \right) \quad (3)$$

where,

$$A_{d_U} = \frac{16\pi^{\frac{5}{2}}}{(2\pi)^{2d_U}} \frac{\Gamma(d_U + \frac{1}{2})}{\Gamma(d_U - 1)\Gamma(2d_U)} \quad (4)$$

In this work we investigate virtual unparticle effects through Moller scattering. We consider the following effective interaction terms, first proposed by Georgi[2]:

$$i\frac{\lambda_V}{\Lambda_U^{d_U-1}}\bar{f}\gamma_\mu f O_U^\mu + i\frac{\lambda_A}{\Lambda_U^{d_U-1}}\bar{f}\gamma_\mu\gamma_5 f O_U^\mu \quad (5)$$

II. CROSS SECTIONS FOR MOLLER SCATTERING

In the presence of the couplings (5), Moller scattering is described by the six t and u-channel tree-level diagrams in Fig.1. Two of them contain unparticle exchange and modify the SM amplitudes.

The polarization summed scattering amplitude for Fig.1 is given by,

$$\begin{aligned} |M|^2 = & g_e^4 A_1 + \frac{g_z^4}{16} A_2 + \frac{g_e^2 g_z^2}{4} A_3 - c_{un}^2 (-t)^{d_U-2} (-u)^{d_U-2} A_4 + g_e^2 c_{un} [(-t)^{d_U-2} A_5 \\ & + (-u)^{d_U-2} A_6] + \frac{g_z^2}{4} c_{un} [(-t)^{d_U-2} A_7 + (-u)^{d_U-2} A_8] + c_{un}^2 (-t)^{2d_U-4} A_9 \\ & + c_{un}^2 (-u)^{2d_U-4} A_{10} \end{aligned} \quad (6)$$

where,

$$A_1 = \frac{2(s^4 + 4ts^3 + 5t^2s^2 + 2t^3s + t^4)}{t^2(s+t)^2} \quad (7)$$

$$\begin{aligned} A_2 = & \frac{1}{(m_z^2 - t)^2(m_z^2 - u)^2} \{ [(c_A^2 - c_V^2)^2 (2t^4 + 4st^3 + 2m_z^4 + 6sm_z^2 + 2stm_z^4 \\ & + 6s^2tm_z^2 + 8s^3t + s^2m_z^4 + 2s^3m_z^2 + 2s^4) + (5c_A^4s^2t^2 + 6c_A^2c_V^2s^2t^2 + 5c_V^4s^2t^2)] \} \end{aligned} \quad (8)$$

$$\begin{aligned} A_3 = & [2(c_A^2(m_z^2s(-s^2 + 3ts + 3t^2) - 2tu(2s^2 + ts + t^2)) - c_V^2(s^2 + ts + t^2)(3sm_z^2 \\ & + 2(s^2 + ts + t^2))) / ((m_z^2 - t)t(s+t)(m_z^2 - u))] \end{aligned} \quad (9)$$

$$A_4 = -2(\lambda_A^4 + 6\lambda_A^2\lambda_V^2 + \lambda_V^4)s^2 \quad (10)$$

$$A_5 = -\frac{2[\lambda_V^2(2s+t)(s^2+ts+t^2) - \lambda_A^2 t(3s^2+3ts+t^2)]}{tu} \quad (11)$$

$$A_6 = -\frac{2[(\lambda_A^2 + \lambda_V^2)s^3 + (\lambda_A^2 - \lambda_V^2)t^3]}{tu} \quad (12)$$

$$A_7 = \frac{1}{(m_z^2 - t)(m_z^2 - u)} \left\{ 2 \left[-(c_A^2 - c_V^2)(\lambda_A^2 - \lambda_V^2) (t^3 + (m_z^2 + 3s)t^2 + st(2m_z^2 + 3s)) \right. \right. \\ \left. \left. + s^2 \left(-2s(c_A \lambda_A - c_V \lambda_V)^2 - ((3\lambda_A^2 + \lambda_V^2)c_A^2 - 8c_V c_A \lambda_V \lambda_A \right. \right. \right. \\ \left. \left. \left. + c_V^2 m_z^2 (\lambda_A^2 + 3\lambda_V^2) \right) \right] \right\} \quad (13)$$

$$A_8 = \frac{1}{(m_z^2 - t)(m_z^2 - u)} \left\{ 2 \left[(c_A^2 - c_V^2)(\lambda_A^2 - \lambda_V^2)(t^3 - m_z^2 t^2) - ((c_A^2 + c_V^2)(\lambda_A^2 + \lambda_V^2) \right. \right. \\ \left. \left. - 4c_V c_A \lambda_V \lambda_A) s^2 (2m_z^2 + s) \right] \right\} \quad (14)$$

$$A_9 = (\lambda_A^2 - \lambda_V^2)^2 (t^2 + 2st) + 2s^2 (\lambda_A^2 + \lambda_V^2)^2 \quad (15)$$

$$A_{10} = s^2 (\lambda_A^4 + 6\lambda_A^2 \lambda_V^2 + \lambda_V^4) + t^2 (\lambda_A^2 - \lambda_V^2)^2 \quad (16)$$

$$c_{un} = \frac{A_{d_U}}{2 \sin(\pi d_U) \Lambda_U^{2d_U-2}}, \quad c_V = -\frac{1}{2} + 2 \sin^2 \theta_W, \quad c_A = \frac{1}{2}, \quad g_z = \frac{g_e}{\sin \theta_W \cos \theta_W} \quad (17)$$

The Mandelstam parameters s , t and u are defined by, $s = (p_1 + p_2)^2$, $t = (p_1 - k_1)^2$ and $u = (p_1 - k_2)^2$. In the cross section calculations we impose a cut $|\cos \theta| < 0.9$ on the scattering angle of one of the final electrons in the C.M. frame.

The behavior of the total cross section as a function of the center of mass energy of the e^-e^- system for $d_U = 1.1, 1.3, 1.5, 1.7$ is shown in Fig.2-5. In the figures we investigate the influence of the scale dimension d_U on the deviations of the total cross sections from their SM value for $\Lambda_U = 1$ TeV and $\Lambda_U = 2$ TeV. We omit a plot of the cross section for $d_U = 1.9$ since it is very close to the SM. One can see from these figures that the deviations of the cross sections grow as the energy increases.

In Fig.2 and Fig.4 we investigate the sensitivity of the cross section to the vector coupling λ_V . So we set $\lambda_V = 1$ and $\lambda_A = 0$. Similarly in Fig.3 and Fig.5 we investigate the axial vector coupling λ_A . We see from these figures that the cross section is more sensitive to λ_V

than λ_A . For instance, in Fig3 the cross section for $d_U = 1.3$ at $E_{cm}=400$ GeV increases by a factor of 3.0 when we compare with its SM value. On the other hand in Fig.2 this increment is a factor of 3.8 for the same scale dimension $d_U = 1.3$. We also see from Fig.2-5 that the deviation of the cross section from its SM value increases with decreasing d_U . This is reasonable since the d_U dependent coefficient c_{un} is inversely proportional to the $(2d_U - 2)$ th power of the energy scale Λ_U (17). Therefore the contribution that comes from the unparticle couplings drastically grow as the d_U decreases. To be precise for $\Lambda_U = 1000$ GeV, $\frac{1}{\Lambda_U^{2d_U-2}}$ grows with a factor of 4000 as d_U decreases from 1.7 to 1.1.

III. CONSTRAINTS ON THE UNPARTICLE COUPLINGS

A more detailed investigation of the unparticle couplings λ_V and λ_A requires statistical analysis. To this purpose we have obtained 95% C.L. limits on λ_V and λ_A using a simple χ^2 analysis at $\sqrt{s}=100, 300, 500$ GeV and integrated luminosity $L_{int}=50$ and 500 fb^{-1} without systematic errors. The χ^2 function is given by,

$$\chi^2 = \left(\frac{\sigma_{SM} - \sigma(\lambda_V, \lambda_A)}{\sigma_{SM} \delta} \right)^2 \quad (18)$$

where $\delta = \frac{1}{\sqrt{N}}$ is the statistical error. N is the number of events. It is given by $N = L_{int}\sigma_{SM}$.

The limits for λ_V and λ_A are given in Tables I-IV. One can see from these tables that the lower and upper bounds on the unparticle couplings are symmetric. The decrease in d_U highly improves the sensitivity limits. The most sensitive results are obtained at $d_U = 1.1$. This value of the scale dimension improves the sensitivity limits of λ_V by a factor of 6 - 16 depending on the energy when we compare with $d_U = 1.7$ for $L_{int}=50$ fb^{-1} . This improvement is a factor of 6 - 14 for the limits of λ_A , depending on the energy.

The energy dependence of the sensitivity limits are interesting. As we have discussed in the previous section the deviation of the cross sections grow as the energy increases. On the other hand the SM cross section and therefore the number of events decreases with the energy. Therefore it is very difficult to predict the behavior of the limits without an explicit calculation. Explicit results are given in the tables.

We see from the tables that the limits for the parameter λ_V are more sensitive than λ_A .

For instance, the sensitivity limit of λ_V for $d_U = 1.1$ is 1.7 times restricted compared to λ_A at $L_{int}=50 \text{ fb}^{-1}$. This factor is 1.75 at $L_{int}=500 \text{ fb}^{-1}$.

-
- [1] H. Georgi, Phys. Rev. Lett. **98**, 221601 (2007).
 - [2] H. Georgi, Phys. Lett. **B650**, 275 (2007).
 - [3] T. Banks and A. Zaks, Nucl. Phys. **B196**, 189 (1982).
 - [4] K. Cheung, W.-Y. Keung and T.-C. Yuan, Phys. Rev. **D76**, 055003 (2007).
 - [5] S. Coleman and E. Weinberg, Phys. Rev. **D7**, 1888 (1973).
 - [6] M. Luo and G. Zhu, Phys. Lett. **B659**, 341 (2008);
C.H. Chen and C. Q. Geng, arXiv:0705.0689 [hep-ph];
Y. Liao, arXiv:0705.0837 [hep-ph];
G.J. Ding and M.L. Yan, arXiv:0705.0794 [hep-ph];
T.M. Aliev, A.S. Cornell and N. Gaur, arXiv:0705.1326 [hep-ph];
X.Q.Li and Z.T. Wei, Phys. Lett. **B651**, 380 (2007);
M.A. Stephanov, Phys. Rev. **D76**, 035008 (2007);
N. Greiner, arXiv:0705.3518 [hep-ph];
S.L. Chen and X.G. He, Phys. Rev. **D76**, 091702 (2007);
H. Davoudiasl, arXiv:0705.3636 [hep-ph];
T.M. Aliev, A.S. Cornell and N. Gaur, JHEP **0707**, (2007);
P. Mathews and V. Ravindran, arXiv:0705.4599 [hep-ph];
S. Zhou, Phys. Lett. **B659**, 336 (2008);
G.J. Ding and M.L. Yan, arXiv:0706.0325 [hep-ph];
C.H. Chen and C.Q. Geng, arXiv:0706.0850 [hep-ph];
Y. Liao and J.Y. Liu, arXiv:0706.1284 [hep-ph];
M. Bander, J.L. Feng, A. Rajaraman and Y. Shirman, arXiv:0706.2677 [hep-ph];
T.G. Rizzo, arXiv:0706.3025 [hep-ph];
S.L. Chen, X.G. He and H.C. Tsai, JHEP **11** (2007) 010;
R. Zwicky, arXiv:0707.0677 [hep-ph];
T. Kikuchi and N. Okada, arXiv:0707.0893 [hep-ph];
R. Mohanta and A.K. Giri, arXiv:0707.1234 [hep-ph];

- C.S. Huang and X.H. Wu, arXiv:0707.1268 [hep-ph];
- N.V. Krasnikov, arXiv:0707.1419 [hep-ph];
- A. Lenz, arXiv:0707.1535 [hep-ph];
- D. Choudhury and D.K. Ghosh, arXiv:0707.2074 [hep-ph];
- T.A. Ryttov and F. Sannino, arXiv:0707.3166 [hep-th];
- A. Delgado, J. R. Espinosa and M. Quiros, arXiv:0707.4309 [hep-ph];
- M. Neubert, arXiv:0708.0036 [hep-ph];
- G. Bhattacharyya, D. Choudhury and D.K. Ghosh, arXiv:0708.2835 [hep-ph];
- Y. Liao, arXiv:0708.3327 [hep-ph];
- A. T. Alan and N. K. Pak, arXiv:0708.3802 [hep-ph];
- L. Anchordoqui and H. Goldberg, arXiv:0709.0678 [hep-ph];
- J. McDonald, arXiv:0709.2350 [hep-ph];
- A. B. Balantekin and K. O. Ozansoy, arXiv:0710.0028 [hep-ph];
- A. T. Alan, N. K. Pak and A. Senol, arXiv:0710.4239 [hep-ph].
- [7] K. Cheung, W.-Y. Keung and T.-C. Yuan, Phys. Rev. Lett. 99, 051803 (2007).

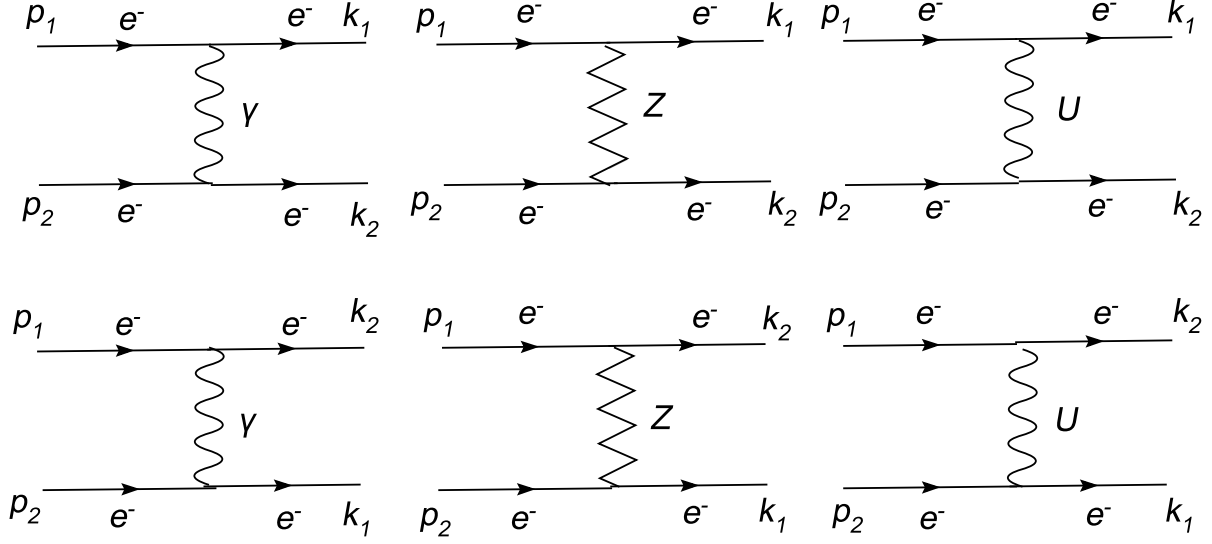


FIG. 1: Tree-level Feynman diagrams for Moller scattering in the presence of the couplings (5).

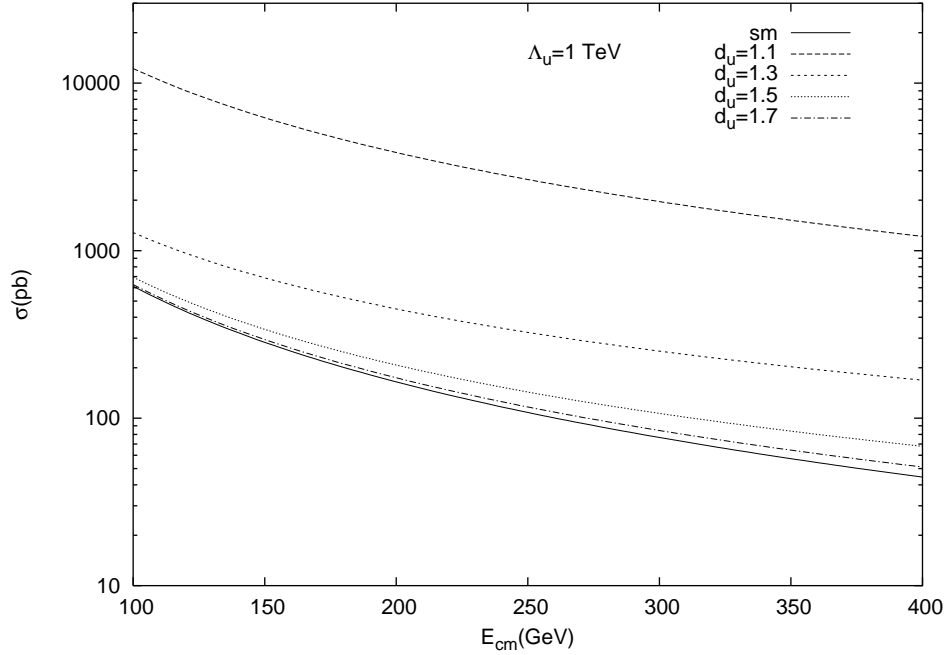


FIG. 2: The total cross section for $\lambda_V = 1$ and $\lambda_A = 0$ as a function of center of mass energy. The legends are for different values of the scale dimension d_U . $\Lambda_U = 1 \text{ TeV}$.

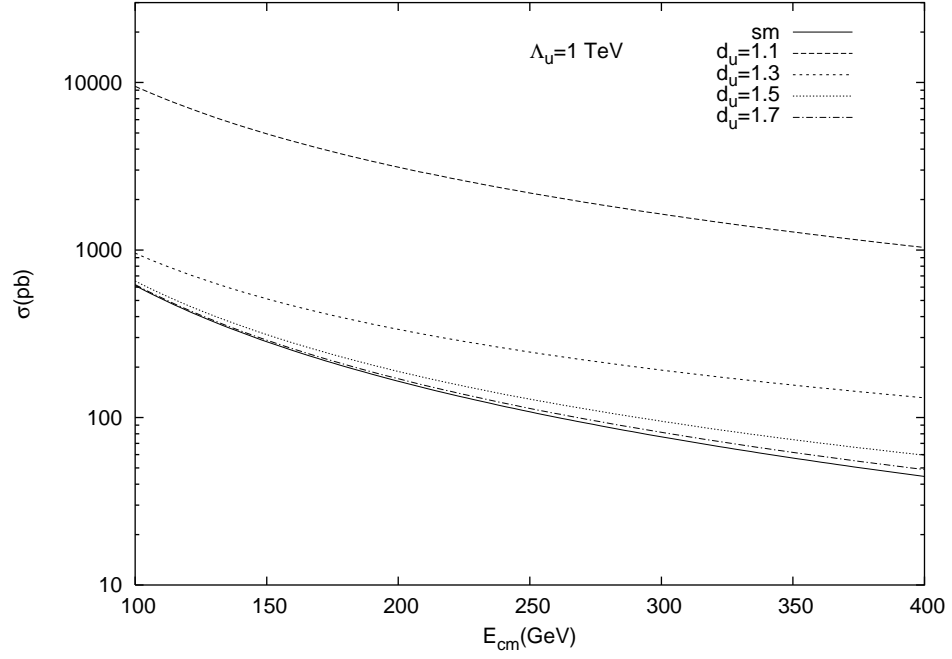


FIG. 3: The same as Fig.2 but for $\lambda_V = 0$ and $\lambda_A = 1$.

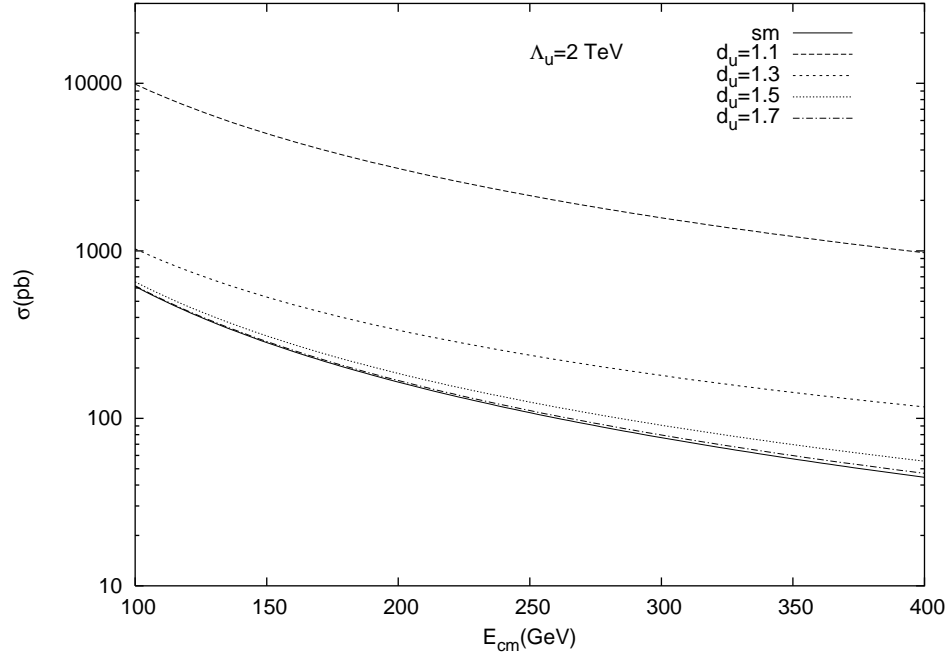


FIG. 4: The same as Fig.2 but for $\Lambda_U = 2$ TeV.

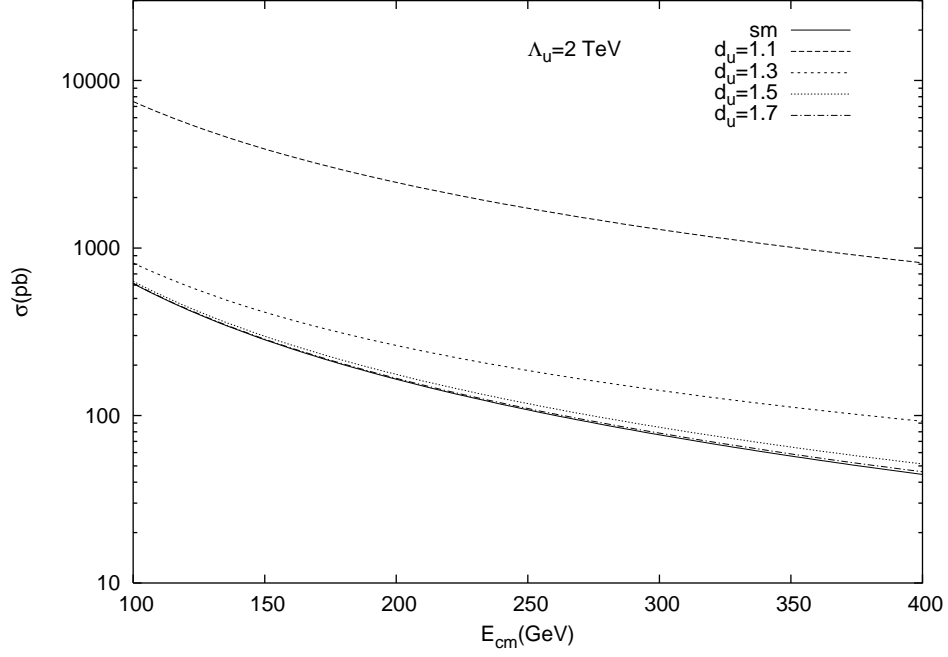


FIG. 5: The same as Fig.3 but for $\Lambda_U = 2$ TeV.

TABLE I: Sensitivity of Moller scattering to λ_V coupling at 95% C.L. for $L_{int} = 50 \text{ fb}^{-1}$ and $\Lambda_U = 1000 \text{ GeV}$.

$\sqrt{s}(\text{GeV})$	$d_u = 1.1$	$d_u = 1.3$	$d_u = 1.5$	$d_u = 1.7$
100	-0.007, 0.007	-0.019, 0.019	-0.046, 0.046	-0.115, 0.115
300	-0.011, 0.011	-0.026, 0.026	-0.052, 0.052	-0.098, 0.098
500	-0.014, 0.014	-0.026, 0.026	-0.048, 0.048	-0.085, 0.085

TABLE II: Sensitivity of Moller scattering to λ_A coupling at 95% C.L. for $L_{int} = 50 \text{ fb}^{-1}$ and $\Lambda_U = 1000 \text{ GeV}$.

$\sqrt{s}(\text{GeV})$	$d_u = 1.1$	$d_u = 1.3$	$d_u = 1.5$	$d_u = 1.7$
100	-0.012, 0.012	-0.030, 0.030	-0.076, 0.076	-0.168, 0.168
300	-0.016, 0.016	-0.035, 0.035	-0.071, 0.071	-0.130, 0.130
500	-0.018, 0.018	-0.034, 0.034	-0.063, 0.063	-0.104, 0.104

TABLE III: Sensitivity of Moller scattering to λ_V coupling at 95% C.L. for $L_{int} = 500 \text{ fb}^{-1}$ and $\Lambda_U = 1000 \text{ GeV}$.

$\sqrt{s}(\text{GeV})$	$d_u = 1.1$	$d_u = 1.3$	$d_u = 1.5$	$d_u = 1.7$
100	-0.004,0.004	-0.012,0.012	-0.032,0.032	-0.080,0.080
300	-0.006,0.006	-0.014,0.014	-0.032,0.032	-0.062,0.062
500	-0.008,0.008	-0.016,0.016	-0.029,0.029	-0.047,0.047

TABLE IV: Sensitivity of Moller scattering to λ_A coupling at 95% C.L. for $L_{int} = 500 \text{ fb}^{-1}$ and $\Lambda_U = 1000 \text{ GeV}$.

$\sqrt{s}(\text{GeV})$	$d_u = 1.1$	$d_u = 1.3$	$d_u = 1.5$	$d_u = 1.7$
100	-0.007,0.007	-0.017,0.017	-0.041,0.041	-0.091,0.091
300	-0.010,0.010	-0.022,0.022	-0.042,0.042	-0.078,0.078
500	-0.010,0.010	-0.019,0.019	-0.035,0.035	-0.055,0.055